





Article

Investigating the Role of *SNAIL* and *ZEB1* Expression in Prostate Cancer Progression and Immune Modulation of the Tumor Microenvironment

William Lautert-Dutra ^{1,†} , Camila Moraes Melo ^{1,†}, Luiz Paulo Chaves ¹, Francisco Cesar Sousa ² , Cheryl Crozier ³, Dan Dion ³, Filipe S. Avante ², Fabiano Pinto Saggioro ⁴, Rodolfo Borges dos Reis ² , Leticia Fröhlich Archangelo ⁵, Jane Bayani ^{3,6} and Jeremy A. Squire ^{1,2,7,*} 

- ¹ Department of Genetics, Faculty of Medicine at Ribeirão Preto, University of São Paulo (FMRP-USP), Ribeirão Preto 14049-900, SP, Brazil; willamlautert@alumni.usp.br (W.L.-D.); camilammelo@alumni.usp.br (C.M.M.); luizpaulocds@alumni.usp.br (L.P.C.)
- ² Division of Urology, Department of Surgery and Anatomy, University of São Paulo (FMRP-USP), Ribeirão Preto 14049-900, SP, Brazil; franciscocesar@alumni.usp.br (F.C.S.); favante@hcrp.usp.br (F.S.A.); rodolforeis@fmrp.usp.br (R.B.d.R.)
- ³ Diagnostic Development, Ontario Institute for Cancer Research, Toronto, ON M5G 0A3, Canada; ccrozier@oicr.on.ca (C.C.); dan.dion@oicr.on.ca (D.D.); jane.bayani@oicr.on.ca (J.B.)
- ⁴ Department of Pathology, University of São Paulo (FMRP-USP), Ribeirão Preto 14049-900, SP, Brazil; fsaggioro@terra.com.br
- ⁵ Department of Cellular and Molecular Biology and Pathogenic Bioagents, Ribeirão Preto Medical School, University of São Paulo (FMRP-USP), Ribeirão Preto 14049-900, SP, Brazil; leticiafa@fmrp.usp.br
- ⁶ Laboratory Medicine and Pathology, University of Toronto, Toronto, ON M5G 1E2, Canada
- ⁷ Department of Pathology and Molecular Medicine, Queen's University, Kingston, ON K7L3N6, Canada
- * Correspondence: squirej@fmrp.usp.br
- † These authors contributed equally to this work.



Citation: Lautert-Dutra, W.; Melo, C.M.; Chaves, L.P.; Sousa, F.C.; Crozier, C.; Dion, D.; Avante, F.S.; Saggioro, F.P.; dos Reis, R.B.; Archangelo, L.F.; et al. Investigating the Role of *SNAIL* and *ZEB1* Expression in Prostate Cancer Progression and Immune Modulation of the Tumor Microenvironment. *Cancers* **2024**, *16*, 1480. <https://doi.org/10.3390/cancers16081480>

Academic Editor: David Wong

Received: 4 March 2024

Revised: 3 April 2024

Accepted: 8 April 2024

Published: 12 April 2024



Copyright: © 2024 by the authors. Licensee MDPI, Basel, Switzerland. This article is an open access article distributed under the terms and conditions of the Creative Commons Attribution (CC BY) license (<https://creativecommons.org/licenses/by/4.0/>).

Simple Summary: We evaluate the downstream effects of the Epithelial-to-Mesenchymal Transition (EMT) transcription factors, *ZEB1* and *SNAIL*, and analyze their potential significance as biomarkers for increased aggressiveness and immune response in prostate cancer (PCa). We used two commercial expression profiling panels to examine a primary PCa cohort ($n = 51$) and identified changes in gene expression linked to downstream pathways associated with biochemical recurrence and increased clinical risk. Genes such as *COL1A1*, *COL1A2*, and *COL3A1*, which are implicated in the tumor microenvironment, and immune-related genes, such as *THY1*, *IRF5*, and *HLA-DRA*, exhibited significant expression level changes. Enrichment analysis identified pathways associated with angiogenesis, TGF-beta, EMT, and UV response in PCa progression. Confirmatory analyses conducted using public domain data demonstrated the downstream impacts of *ZEB1* and *SNAIL* on pathways and immune responses, highlighting their potential influence on immune modulation in PCa. Future treatment strategies aimed at modulating EMT may enhance immune cell infiltration toward an anti-tumorigenic phenotype.

Abstract: Prostate cancer (PCa) is an immunologically cold tumor and the molecular processes that underlie this behavior are poorly understood. In this study, we investigated a primary cohort of intermediate-risk PCa ($n = 51$) using two NanoString profiling panels designed to study cancer progression and immune response. We identified differentially expressed genes (DEGs) and pathways associated with biochemical recurrence (BCR) and clinical risk. Confirmatory analysis was performed using the TCGA-PRAD cohort. Noteworthy DEGs included collagens such as *COL1A1*, *COL1A2*, and *COL3A1*. Changes in the distribution of collagens may influence the immune activity in the tumor microenvironment (TME). In addition, immune-related DEGs such as *THY1*, *IRF5*, and *HLA-DRA* were also identified. Enrichment analysis highlighted pathways such as those associated with angiogenesis, TGF-beta, UV response, and EMT. Among the 39 significant DEGs, 11 (28%) were identified as EMT target genes for *ZEB1* using the Harmonizome database. Elevated *ZEB1* expression correlated with reduced BCR risk. Immune landscape analysis revealed that *ZEB1* was associated with increased immunosuppressive cell types in the TME, such as naïve B cells and M2 macrophages.

Increased expression of both *ZEB1* and *SNAIL* was associated with elevated immune checkpoint expression. In the future, modulation of EMT could be beneficial for overcoming immunotherapy resistance in a cold tumor, such as PCa.

Keywords: biomarkers; immune evasion; bioinformatics; gene signatures; immunotherapy; extracellular matrix; transcriptomics; collagens; immune checkpoint proteins; digital flow cytometry

1. Introduction

Prostate cancer (PCa) is the second most common cancer in men and the fifth cause of cancer-related deaths worldwide [1,2]. The disease course is often favorable, but unfortunately, 20–30% of patients with localized disease will eventually progress and develop advanced disease and metastasis [3]. Once resistance to androgen deprivation therapy develops, there are limited chemotherapy choices available to control the progression [4], but recently there has been increasing interest in the use of immunotherapy in the advanced setting.

The effect of checkpoint blockade therapy in metastatic PCa has been disappointing, with just 5–10% of patients responding [5,6]. These poor results are primarily thought to be because PCa is an immunologically cold or excluded tumor [7,8]. In various solid tumors, the presence of immune infiltration within the tumor microenvironment (TME) has been associated with improved immune control and a better prognosis [9].

The TME is the cellular ecosystem that surrounds a tumor, and it includes immune cells, the extracellular matrix (ECM), blood vessels, and other cells, such as cancer-associated fibroblasts (CAFs) that may modulate the composition of the TME. Studies of the immune content in PCa have resulted in inconsistent findings, with some indicating that elevated T cell levels within the TME correlate with improved prognosis [10], while others suggest the opposite effect [11]. The variation in immune infiltration likely contributes to the observed differences in anti-cancer immune responses in PCa [12,13].

Epithelial–mesenchymal transition (EMT) mechanisms can profoundly influence the TME [14]. The EMT is a molecular mechanism associated with tumor progression and acquisition of heterogeneity in advanced cancers [15]. EMT-inducing transcriptional regulators, such as *TWIST*, *SNAIL*, *SNAIL2*, *ZEB1*, and *ZEB2*, exert their phenotypic changes in tumors by modulating the expression of epithelial markers and activating the expression of mesenchymal markers [14]. These downstream regulatory changes in gene expression occur through their direct binding to the promoters of target genes involved in cell adhesion and polarity, leading to loss of cell–cell adhesion, remodeling of the cytoskeleton, and acquisition of migratory and invasive properties characteristic of mesenchymal cells [16].

Zinc finger E-box binding homeobox 1 (*ZEB1*) is an established EMT transcription factor whose expression in PCa is associated with more aggressive disease and chemoresistance [17]. Similarly, Snail family transcriptional repressor 1 (*SNAIL*) is the main promoter of EMT in PCa [18], and its expression is associated with a higher Gleason score [19] and increased cell migration [20].

EMT-driven alterations to the TME can lead to resistance to immunotherapy [21,22]. *TGF- β* signaling is integral to the epithelial phenotype and downstream effects induce changes in the stromal environment to facilitate tumor progression [23]. The expression of *TGF- β* interacts with both the Snail and *ZEB1* proteins to influence cancer–TME crosstalk related to immune evasion [24–26].

The prognostic role of downstream EMT transcriptomics derived from PCa primary intermediate-risk tumors has not previously been investigated in the context of the immune landscape of the TME. In this study, we analyzed the influence of altered *ZEB1* and *SNAIL* expression levels on cancer progression using a retrospective cohort of 51 intermediate-risk PCa tumors from FMRP-USP, Brazil. We determined how downstream changes in gene expression related to each transcription factor could lead to PCa progression changes and

immune pathway activities. We used two NanoString mRNA panels (PanCancer Pathway and Immune Profiling) to quantify gene expression levels across the cohort to identify differentially expressed genes (DEGs) and pathways linked to the EMT and progression in intermediate-risk PCa. Our findings indicate that changes in *ZEB1* and *SNAIL* expression in PCa are associated with the induction of DEGs and downstream pathways that influence the TME and may facilitate immune evasion during tumor progression.

2. Materials and Methods

2.1. Tumor Cohort

The Faculty of Medicine at the Ribeirão Preto (FMRP) cohort comprised 51 primary prostate cancer samples obtained via radical prostatectomy, in accordance with the National Comprehensive Cancer Network (NCCN) clinical practice guidelines [27], at the Urology Division of the Department of Surgery and Anatomy, FMRP-USP, Brazil, between 2007 and 2015 (Table S1). Transcriptomic data derived from this cohort were recently included in another publication by our group [28]. Smaller prostates were submitted for pathological assessment in their entirety according to the guidelines of the American College of Pathology. In cases where larger glands were partially sampled, we followed the protocol by submitting the entire tumor if grossly visible, along with the tumor, surrounding periprostatic tissue, and margins, including the entire apical and bladder neck margins. Additionally, we included the junction of each seminal vesicle with the prostate proper. If there was no grossly visible tumor, a systematic sampling strategy was used. This involved taking slices from the posterior aspect of each transverse section, along with a mid-anterior block from each side. Additionally, we submitted samples including the entire apical and bladder neck margins, as well as the junction of each seminal vesicle with the prostate. Biochemical recurrence (BCR) was defined as PSA > 0.2 ng/mL within six months post radical prostatectomy. To assess the likelihood of prostate cancer recurrence after initial surgery, we utilized the Cancer of The Prostate Risk Assessment Score (CAPRA-S) [29]. This scoring system incorporates various clinical and pathological factors, such as pre-treatment PSA level, pathological Gleason score, surgical margin, extracapsular extension, seminal vesicle invasion, and lymph node invasion. CAPRA-S provides a relative risk assessment for biochemical progression, ranging from 1 to 12. For this study, patients with low CAPRA-S scores were those with values between 0 and 2, those with intermediate scores had CAPRA-S scores ranging from 3 to 5, and those with high scores had CAPRA-S scores between 6 and 12. Patient outcome data were collected to the last follow-up date. This retrospective study was approved by the Ethics Committee in Research of Hospital of Ribeirão Preto, São Paulo, Brazil (HCRP), numbers CAAE 60032122.8.0000.5440 and CAAE 43277221.0.0000.5440, and the Ethics Board of the University of Toronto (Protocol 00043323).

2.2. RNA Isolation

RNA extraction was performed on tissues containing tumor-rich areas, which were previously identified and marked by a pathologist (FPS) to represent the highest Gleason pattern. Serial 5 µm formalin-fixed paraffin-embedded (FFPE) tissue was processed at the Ontario Institute for Cancer Research, Toronto, Canada (OICR), using extraction methods described in previous studies [30,31].

2.3. Transcription Analysis

RNA profiling was performed using both the NanoString PanCancer and the Immune Profiling Panels (NanoString Technologies Inc., Seattle, WA, USA) [32] according to the manufacturer's instructions. Briefly, RNA profiling using the NanoString methodology relies on digital molecular barcoding and direct hybridization to quantify gene expression levels across multiple genes simultaneously. This methodology has been shown to offer high sensitivity, specificity, and the ability to analyze gene expression patterns from small amounts of RNA, as described previously [33]. The NanoString PanCancer panel comprises 730 genes involved in the cancer progression processes, such as angiogenesis, extracellular matrix remodeling (ECM), EMT, and metastasis. The Immune Profiling Panel comprises

730 immune response genes specifically optimized for immuno-oncology investigative research. There are 130 endogenous genes common between the 2 transcriptional panels, yielding 1200 unique transcripts available for interrogation. Raw expression data from both panels were loaded in nSolver software v4.0 (NanoString Technologies) to perform the quality control (QC) analysis and to build the transcript matrix for downstream analysis. Pearson correlation analysis was performed for the 160 genes in common between the panels and was used to assess reproducibility and identify any potential panel bias. The majority of the 160 genes common to both panels showed a consistent positive correlation between the panels, indicating that gene expression analyses by each panel were reproducible (Supplementary Figure S1). For initial differential expression, we used DESeq2 v1.34.0 with BCR and risk factor as the design factors [34]. We conducted overrepresentation enrichment analysis (ORA) and Gene Set Enrichment Analysis (GSEA) on the differential expressed genes utilizing the clusterprofiler v4.0 with Kyoto Encyclopedia of Genes and Genomes (KEGG) pathways [35]. Additionally, we categorized the expression levels of *ZEB1* and *SNAIL1* into quartiles for each gene. These categorical data allowed us to classify patient gene expressions as either “low” (below Q3) or “high” (above Q3) for *ZEB1* and *SNAIL1* [28]. We then used the classification status of *ZEB1* and *SNAIL1* as the design factor for the transcriptome analysis as described earlier. For validation purposes, we utilized RNA-seq data from the prostate adenocarcinoma cohort in The Cancer Genome Atlas (PRAD-TCGA, $n = 420$) [36]. We compared the effects of dichotomized expression levels of *ZEB1* and *SNAIL1* in this public domain cohort.

2.4. Digital Cytometry Analysis

To quantify the immune cell composition in the TME of tumors having a high expression of *ZEB1* and *SNAIL1*, we used expression data from TCGA-PRAD [36] analyzed using the digital cytometry resource CIBERSORTx [37]. This algorithm estimates the relative immune abundance in the TME using a “signature matrix” containing validated leukocyte expression data from 22 human hematopoietic cell phenotypes (LM22).

2.5. Statistical Analysis

The data processing and downstream analysis for transcriptome data were completed in Rstudio software (R Foundation for Statistical Computing, R v4.1.2 “Bird Hippie”). Multiple unpaired *t*-tests were assessed to calculate the statistical significance using the GraphPad Prism 9.3.0 software for CIBERSORT data. Genes were considered differentially expressed when log2 fold change > 0.5 for the NanoString PanCancer and Immune Profiling Panels, and a more rigorous threshold of > 0.58 was used for validation comparisons with the TCGA-PRAD, with p-adjusted (FDR) < 0.05 . For the enrichment analysis, we used a cutoff value of 0.05 to consider the ORA of Molecular Signatures Database (MsigDB) Hallmarks. Kaplan–Meier estimates of BCR-free survival were computed using the survival package v3.4.0. Figure S1 illustrates the general workflow of this work (Supplementary Figure S2).

3. Results

3.1. Identification of DEGs and Pathways Associated with BCR and Clinical Risk

The NanoString PanCancer and the Immune Profiling Panel were developed to cover cancer-related biological functions and features related to adaptive and innate immune response genes. Using both panels, we examined the DEGs (log2 fold change > 0.5) to determine the impact of downstream changes in gene expression on PCa progression through outcome and immune evasion pathways.

In the first phase of our transcriptomic analysis, we investigated DEGs within the FMRP cohort stratified by CAPRA-S and BCR status. Patients with either a CAPRA-S intermediate or a CAPRA-S high relative risk were grouped together as “High”, while the remaining patients identified as low-risk CAPRA-S, were defined by the “Low” group.

Tables 1 and 2 summarize the significantly associated DEGs with BCR and CAPRA-S determined using the PanCancer panel and Immune Panel, respectively. Many of the DEGs

identified in this analysis have been previously reported as prognostic biomarkers in PCa or have been published as potential markers of immune response in various cancers.

Table 1. Ranked list of the DEGs associated with BCR and CAPRA-S based on the PanCancer Panel using the FMRP cohort. The roles of each of the top-ranking DEGs in the cancer progression and PCa literature are shown with specific citations (if available). Adjusted *p*-value < 0.05 and a log2 fold change > 0.5.

	Gene	Log2 FC	padj	Protein	Role in Progression and Biology of PCa	Citations
BCR	<i>COL1A1</i>	0.876	>0.001	collagen type I alpha 1 chain	Collagens contribute to the ECM, which are the major structural components of the TME. <i>COL1A1</i> , <i>COL1A2</i> , and <i>COL3A1</i> expression in CAFs have been associated with the EMT. <i>COL1A1</i> expression is upregulated in PCa stromal cells and was associated with a worse prognosis in PCa.	[38,39]
	<i>COL3A1</i>	0.879	>0.001	collagen type III alpha 1 chain	<i>COL3A1</i> interacts with fibronectin. Increased expression of <i>COL3A1</i> in PCa activates other pro-tumorigenic genes and pathways, such as the Wnt/beta-catenin. <i>COL3A1</i> expression is associated with higher Gleason scores, higher PSA levels, and a higher likelihood of lymph node involvement.	[38]
	<i>COL1A2</i>	0.596	>0.001	collagen type I alpha 2 chain	<i>COL1A2</i> expression is associated with higher Gleason scores.	[40]
	<i>COL5A2</i>	0.479	>0.001	collagen type V alpha 2 chain	<i>COL5A2</i> expression has been associated with increased tumor cell invasion and resistance to androgen deprivation therapy.	[40]
	<i>SFRP2</i>	0.761	0.004	secreted frizzled-related protein 2	<i>SFRP2</i> affects TME by regulating Wnt signaling and influencing tumor angiogenesis.	[41,42]
	<i>THBS4</i>	0.852	0.007	thrombospondin 4	<i>THBS4</i> affects cancer stem cell-like properties in PCa by its regulation of the PI3K/Akt pathway.	[43]
	<i>INHBA</i>	0.766	0.008	inhibin beta A subunit	<i>INHBA</i> (Activin A) activates NF-κB and is associated with a higher Gleason score PCa.	[44,45]
	<i>WNT2B</i>	0.567	0.02	Wnt family member 2B	<i>WNT2B</i> is regulated by lncRNAs to influence the EMT in PCa.	[46]
	<i>SFRP4</i>	0.7349	0.03	secreted frizzled-related protein 4	<i>SFRP4</i> predicts BCR in PCa and is associated with the EMT.	[47]

Table 1. Cont.

	Gene	Log2 FC	padj	Protein	Role in Progression and Biology of PCa	Citations
CAPRA-S	<i>NOTCH3</i>	0.6882	>0.001	notch 3	<i>NOTCH1-4</i> expression was associated with disease progression, prognosis, and immune cell infiltration.	[48]
	<i>BMP8A</i>	0.8167	0.006	bone morphogenetic protein 8a	BMPs are members of the TGF-beta family and are thought to be involved in PCa bone metastasis.	[49]
	<i>CHEK1</i>	0.8851	0.01	checkpoint kinase 1	<i>CHEK1 (CHK1)</i> is associated with DNA damage response and AR signaling.	[50]
	<i>COL3A1</i>	0.8822	0.01	collagen type III alpha 1 chain	see above	
	<i>NTRK1</i>	−1.045	0.01	neurotrophic receptor tyrosine kinase 1	<i>NTRK1</i> downregulation is associated with reduced TILs in the TME of PCa and poor prognosis.	[51]
	<i>FN1</i>	0.686	0.01	fibronectin 1	<i>FN1</i> is a key component of the ECM, and the TME is associated with collagens and CAFs.	[52]
	<i>JAG1</i>	0.697	0.02	jagged 1	<i>JAG1</i> upregulation results in increased inflammatory foci in the TME of tumors in <i>Pten</i> -deficient mice.	[53]
	<i>INHBA</i>	0.905	0.02	inhibin beta A subunit	See above.	
	<i>CD14</i>	0.592	0.04	CD14 molecule	<i>CD14</i> is mostly expressed in macrophages.	--
	<i>GAS1</i>	−0.606	0.04	growth arrest-specific 1	<i>GAS1RR</i> (an immune-related enhancer RNA) represses <i>GAS1</i> and is associated with BR-free survival in PCa.	[54]
	<i>SOX17</i>	−0.561	0.04	SRY-box 17	<i>SOX17</i> and Notch's axis associated with enzalutamide resistance in CRPC models.	[55]

Table 2. Ranked list of the DEGs associated with BCR and CAPRA-S based on the Immune Profiling Panel using the FMRP. The roles of each of the top-ranking DEGs in immune oncology and the PCa literature are shown with specific citations (if available). Adjusted *p*-value < 0.05 and a log2 fold change > 0.5.

	Gene	Log2 FC	padj	Protein	Role in Immune Oncology and PCa	Citations
BCR	<i>COL3A1</i>	1.027	>0.001	collagen type III alpha 1 chain	See Table 1.	
	<i>ENG</i>	0.556	0.001	endoglin	Endoglin (sCD105) in plasma associated with aggressive PCa.	[56]
	<i>CXCL14</i>	1.291	0.002	C-X-C motif chemokine ligand 14	<i>CXAL14</i> expression associated with outcome in PCa.	[57]

Table 2. Cont.

	Gene	Log2 FC	padj	Protein	Role in Immune Oncology and PCa	Citations
CAPRA-S	<i>SH2D1A</i>	−0.045	0.005	SH2 domain containing 1A	Stimulation factor for T and B cells.	--
	<i>IRF5</i>	0.478	0.01	interferon regulatory factor 5	IRF5 expression used for BCR prediction in PCa.	[58]
	<i>SYK</i>	0.506	0.02	spleen associated tyrosine kinase	Associated with metastatic PCa.	[59]
	<i>ICOS</i>	0.231	0.03	inducible T cell costimulator	ICOS + Treg cells exert immunosuppressive effects.	--
	<i>CXCL10</i>	1.549	0.003	C-X-C motif chemokine ligand 10	CXCL10 co-expression with CXCR3 is a predictor of metastatic recurrence.	[60]
	<i>FCGR2A</i>	0.669	0.003	Fc fragment of IgG receptor IIa	Expressed in macrophages, neutrophils, and other immune cells.	--
	<i>MSR1</i>	0.804	0.003	macrophage scavenger receptor 1	Helpful as an additional diagnostic biomarker for PCa.	[61]
	<i>CD84</i>	0.618	0.004	CD84 molecule	Expressed in numerous immune cell types.	--
	<i>KIR Activating Subgroup 1</i>	−0.98	0.01	killer cell immunoglobulin-like receptors	KIRs expressed in NK and T cells.	[62]
	<i>THY1</i>	0.631	0.01	Thy-1 cell surface antigen	<i>THY1</i> overexpressed in PCa-associated fibroblasts.	[63]
	<i>SIGIRR</i>	0.459	0.02	single Ig and TIR domain containing	<i>TLR4</i> and <i>IL-1R</i> -mediated NF-κB activation associated with BCR.	[64]
	<i>HLA-DRA</i>	0.636	0.02	major histocompatibility complex, class II, DR alpha	Antigen presentation in the TME.	[65]
	<i>NRP1</i>	0.534	0.02	neuropilin 1	Androgen-repressed gene upregulated by ADT in advanced PCa.	[66]
	<i>COL3A1</i>	0.865	0.03	collagen type III alpha 1 chain	See Table 1.	
	<i>IFNL1</i>	−0.66	0.04	interferon lambda 1	Interferon lambda 1 is involved in antiviral immune defense.	--
	<i>CD14</i>	0.528	0.04	CD14 molecule	<i>CD14</i> is mostly expressed in macrophages.	--
	<i>FN1</i>	0.570	0.04	fibronectin 1	See Table 1.	

Volcano plot analysis of the significantly altered DEGs associated with BCR included the overexpression of *SFRP2*, *THBS4*, *INHBA*, *WNT2B*, and *SFRP4* (Figure 1A), as well as *ENG*, *CXCL14*, and *SYK* (Figure 1B) amongst the “Low” CAPRA-S group. Similarly, the “High” CAPRA-S group exhibited a substantial number of DEGs (Figure 1C,D). Association with CAPRA-S showed increased expression of *BMP8A*, *CHEK1*, *FN1*, *COL3A1*, *JAG1*, *CD14*, *INHBA*, and *PDGFRB* (PanCancer) and *FCGR2A*, *CD84*, *MSR1*, *CXCL10*, *THY1*, *HLA-DRA*, *COL3A1*,

NRP1, *CD14*, and *FN1* (Immune Panel). Reduced expression of *NTRK1*, *GAS1*, and *SOX17* (PanCancer) and *KIR_Activating_Subgroup 1* and *IFNL1* (Immune Panel) was also identified. Amongst the overlapping genes between panels, increased expression of *CD14*, *FN1*, and *COL3A1* were independently detected and associated with high CAPRA-S (Figure 1E,F).

The last part of our investigation was to identify pathways based on ORA and GSEA analyses of the DEGs identified. Enrichment analysis revealed pathways related to angiogenesis, and TGF-beta, EMT, and UV response were associated with progression and immune response in the FMRP cohort (Supplementary Table S2). Underscoring the importance of the EMT in PCa progression, 11 (28%) of the 39 DEGs (Figure 1F) associated with BCR or CAPRA-S in our cohort were identified as target genes for the EMT transcription factor *ZEB1* [67].

Thus, our initial analyses revealed DEGs associated with immune responses and progression, some of which are regulated by the EMT driver *ZEB1*. Additionally, genes implicated in the remodeling of the TME, including members of the collagen family (*COL1A*, *COL1A2*, *COL3A1*, *COL5A2*) [38], fibronectin (*FN1*) [52], and *SFRP4* [47], were identified as putative markers of PCa progression. These findings, in conjunction with existing published data (as reviewed in [68]), highlight the potential impact of EMT mechanisms on modulating the immune TME during the progression of PCa.

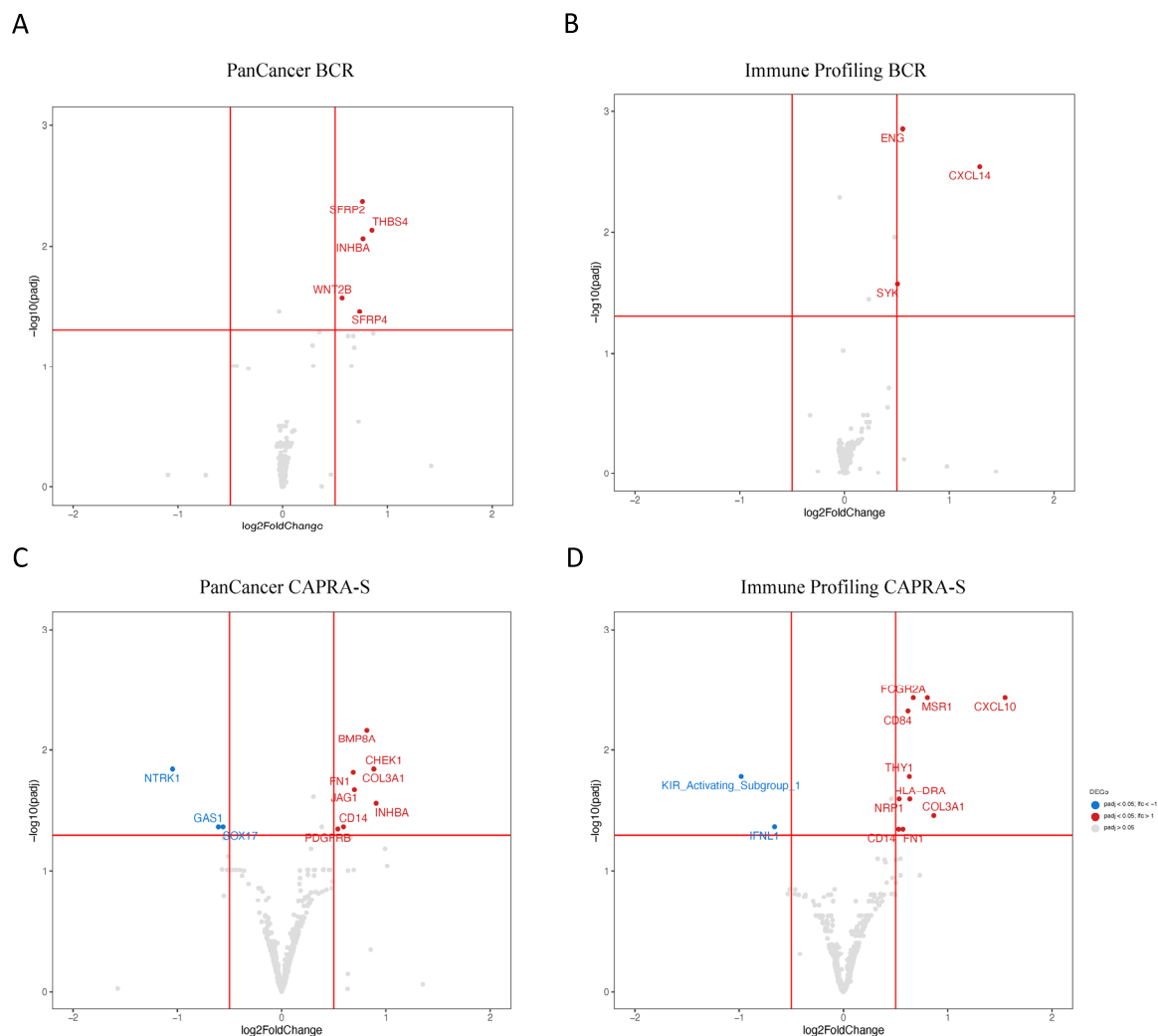
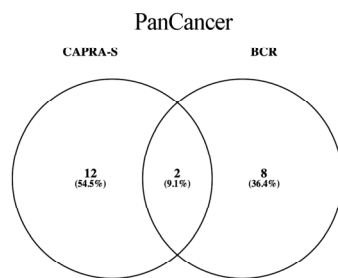


Figure 1. Cont.

E

**High CAPRA-S:**

NOTCH3; **BMP8A*; *CHEK1*; **NTRK1*; *FN1*; **JAG1*; **DNMT1*;
CAPN2; **CD14*; **GAS1*; *SOX17*; *PDGFRB*

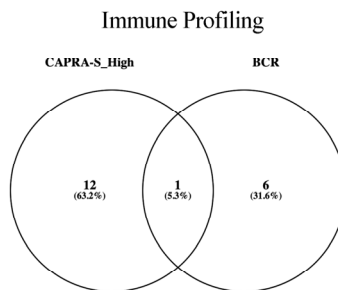
BCR:

**COL1A1*; *COL1A2*; *COL5A2*; *SFRP2*; *THBS4*; **WNT2B*;
CACNG6; *SFRP4*

High Capra-S + BCR:

COL3A1; *INHBA*

F

**High CAPRA-S:**

CXCL10, *FCGR2A*, *MSR1*, *CD84*,
KIR_Activating_Subgroup_1, *THY1*, **SIGIRR*, *HLA-DRA*,
NRP1, *IFNL1*; **CD14*, *FN1*

BCR:

ENG, *CXCL14*, *SH2D1A*; **IRF5*; **SYK*, *ICOS*

High Capra-S + BCR:

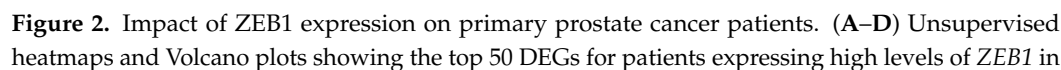
COL3A1

Figure 1. NanoString profile of primary prostate cancer patients. (A–D) Volcano plots of the DEGs stratified by BCR and CAPRA-S status for both transcriptome panels. (E,F) Venn diagrams represent the intersection of the DEGs from BCR and CAPRA-S for both transcriptome panels. The list of 39 significantly associated DEGs from both comparisons is displayed on the right side of both panels. Eleven of these DEGs (*COL1A1*, *WNT2B*, *BMP8A*, *NTRK1*, *JAG1*, *DNMT1*, *CD14*, *GAS1*, *SIGIRR*, *IRF5*, and *SYK*) marked with * were identified as target genes for the EMT transcription factor *ZEB1* using the ENCODE transcription factor dataset that has all 8646 target genes of *ZEB1* based on ChIP-seq [67]. Both clinical comparisons used no BCR and low CAPRA-S scores as references from the FMRP cohort. Adjusted *p*-value < 0.05 and a log2 fold change > 0.5. Data were plotted using *ggplot2* and Venny (<https://bioinfogp.cnb.csic.es/tools/venny/index.htm>, accessed on 5 December 2023).

3.2. Downstream Effects of *ZEB1* and *SNAI1* Expression

The dichotomization of *ZEB1* and *SNAI1* gene expression levels was based on quartile (Q) values, with patients classified as “low” defined as below Q3 compared to those classified as “high” being above Q3. Our objective was to establish a classification system for the DEG patterns linked to the transcriptional activity of these two EMT drivers and the potential impact on downstream pathways involved in PCa progression. DEGs derived from the analysis of both panels classified by *ZEB1* and *SNAI1* expression levels are shown in Supplementary Table S3.

Using an unsupervised approach, potential relationships amongst samples based on *ZEB1* expression profiles were performed and summarized in Figure 2A,B (PanCancer) and Figure 2C,D (Immune Profiling). A distinct cluster of DEGs associated with high *ZEB1* expression was revealed in the PanCancer panel (Figure 2A), identified by a significantly increased expression of *LEFTY2*, *LTBP1*, *WNT2B*, *SFRP2*, *PDGFRB*, *COL5A1*, *JAG1*, *SMO*, *HHIP*, and *LEF1* (Figure 2B), as well as several under-expressed genes, including *EFNA2*, *NODAL*, *UTY*, *IL8*, *IL13*, *IL24*, and *IL11*. Across the genes in the Immune Panel (Figure 2C), a large cluster of DEGs associated with high *ZEB1* expression was observed, including an increased expression of *CKCLF*, *PSEN2*, *JAK1*, *PDGFRB*, *LRP1*, *CD58*, *PECAM1*, *IFITM1*, *SPACA3*, *MEFV*, *HLA-DPA1*, *FUT7*, *LY86*, *CXCL10*, *LY96*, *CD84*, *HLA-DPB1*, and *HLA-DRA* (Figure 2D). Similarly, an under-expressed cluster of genes included *IL8*, *TNFSF11*, *CXCR1*, and *IL11* (Figure 2D). Pathway analysis of the up- and downregulated DEGs was performed using ORA. *ZEB1* expression was associated with allograft rejection, inflammatory response, interferon-alpha and interferon-gamma response, EMT, IL-2/STAT5, IL-6/JAK/STAT3, WNT/beta-catenin (Supplementary Table S4).



the FMRP cohort ($n = 51$). Because the display software is limited by the area available for visualizing the top genes, not all significantly expressed DEGs are depicted in the Volcano plots. (E) The Kaplan–Meier plot shows that a low level of *ZEB1* expression is associated with a reduced recurrence-free interval (log-rank test, $p = 0.04$). Adjusted p -value < 0.05 and a log2 fold change > 0.5 . Data were plotted using *heatmap* and *ggplot2*.

The elevated *ZEB1* expression demonstrated a statistically significant association with a reduced risk of BCR for our cohort of intermediate-risk PCa, as determined by Kaplan–Meier analysis, (log-rank test $p = 0.04$) (Figure 2E). This observation aligns with previous findings in which reduced *ZEB1* expression was associated with aggressive disease in PCa [69].

Transcriptome analysis based on the dichotomization of *SNAI1* uncovered several DEGs illustrated in Figure 3A,B (PanCancer) and Figure 3C,D (Immune Profiling). Results from the PanCancer panel demonstrated clustering associated with high *SNAI1* expression, revealing a reduced expression of *HOXA11*, *GRIN1*, *SOST*, *CALML5*, and *NODAL* (Figure 3A,B). Significantly overexpressed genes include *RUNX1*, *ETS2*, *IL1B*, *LIF*, and *IL8*. Similarly, DEGs related to *SNAI1* expression from the Immune Profiling Panel included the overexpression of *CD274* (*PDL1*), *IL1B*, and *TNFRSF9* (Figure 3C,D).

Enrichment analysis of DEGs identified pathways, including TNF-alpha via NF-kB, hypoxia, p53, and PI3K/AKT/mTOR, in addition to those identified in our analysis linked with *ZEB1* expression, including IL-2/STAT5, IL-6/JAK/STAT3, EMT, and interferon-alpha and interferon-gamma response (Table 3). Kaplan–Meier analysis revealed no significant association between *SNAI1* and BCR-free survival (*SNAI1* high vs. low expression, log-rank test, $p = 0.85$) (Figure 3E).

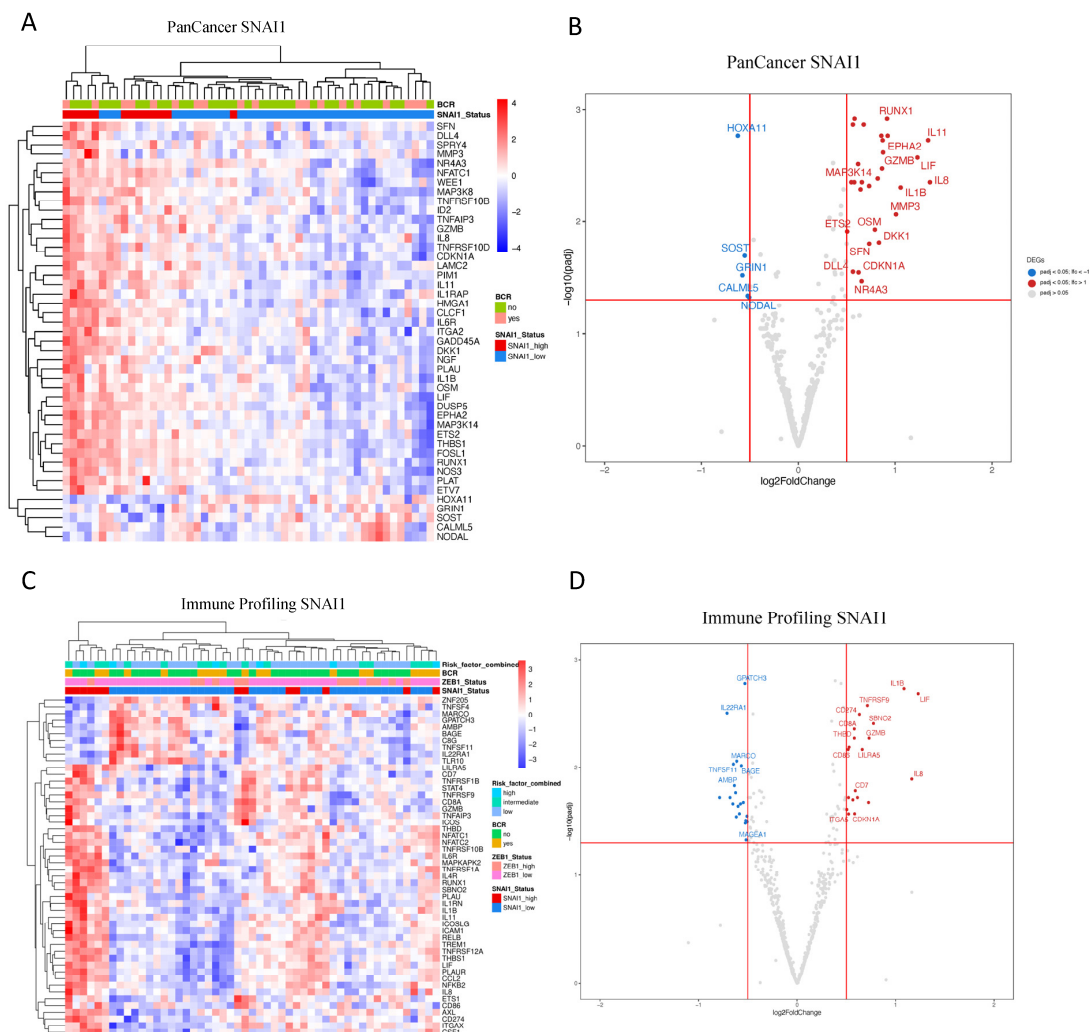


Figure 3. Cont.

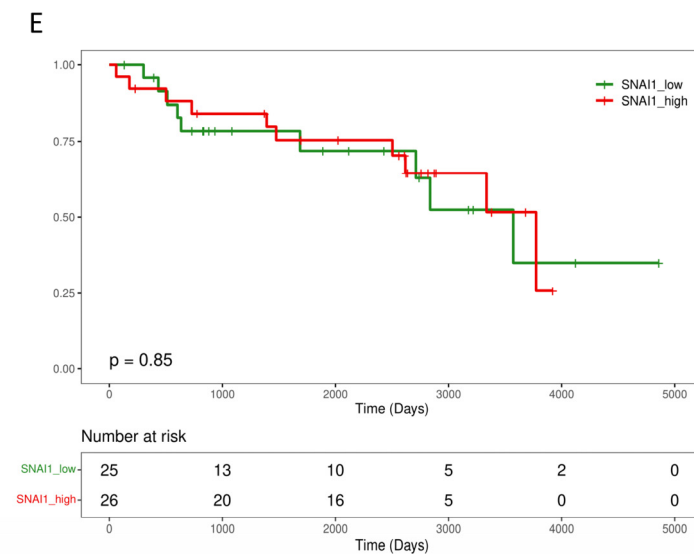


Figure 3. Impact of SNAI1 expression on primary prostate cancer patients. (A–D) Unsupervised heatmaps and Volcano plots showing the top 50 DEGs for patients expressing high levels of *SNAI1* in the FMRP cohort ($n = 51$). (E) The Kaplan–Meier plot shows that the recurrence interval is not affected by levels of *SNAI1* (log-rank test, $p = 0.85$) in the FMRP cohort. Adjusted p -value < 0.05 and a \log_2 fold change > 0.5 . Data were plotted using *pheatmap*.

Table 3. Enrichment analysis from DEGs associated with *SNAI1* High expression in the HC-FMRP cohort. List of ORA enriched pathways using MSigDb Hallmark’s terms for DEGs associated with high expression of *SNAI1*. The analysis used patients with low expression of *SNAI1* as a reference.

Term	Adjusted p -Value	Genes
Immune Profiling		
TNF-alpha Signaling via NF-kB	>0.001	<i>EGR2</i> ; <i>CDKN1A</i> ; <i>CSF1</i> ; <i>CD80</i> ; <i>TNFRSF9</i> ; <i>LIF</i> ; <i>PLAUR</i> ; <i>TNFAIP3</i> ; <i>NFKB1</i> ; <i>ICAM1</i> ; <i>NFKB2</i> ; <i>REL</i> ; <i>NFKBIA</i> ; <i>BCL6</i> ; <i>PLAU</i> ; <i>IL1B</i> ; <i>REL</i> ; <i>CCL2</i> ; <i>ICOSLG</i> ; <i>CD44</i>
Inflammatory Response	>0.001	<i>CDKN1A</i> ; <i>IL4R</i> ; <i>CSF1</i> ; <i>TNFRSF9</i> ; <i>IL10RA</i> ; <i>LIF</i> ; <i>PLAUR</i> ; <i>ICAM4</i> ; <i>TNFRSF1B</i> ; <i>NFKB1</i> ; <i>ICAM1</i> ; <i>NFKBIA</i> ; <i>MARCO</i> ; <i>IRAK2</i> ; <i>AXL</i> ; <i>IL1B</i> ; <i>IRF7</i> ; <i>CCL2</i> ; <i>ITGA5</i> ; <i>ICOSLG</i>
Allograft Rejection	>0.001	<i>CD86</i> ; <i>CCR1</i> ; <i>IL11</i> ; <i>IL4R</i> ; <i>CSF1</i> ; <i>CD80</i> ; <i>LIF</i> ; <i>GZMB</i> ; <i>ETS1</i> ; <i>ICAM1</i> ; <i>NCR1</i> ; <i>CD8A</i> ; <i>IL1B</i> ; <i>IL9</i> ; <i>CD7</i> ; <i>IRF7</i> ; <i>STAT4</i> ; <i>CCL2</i> ; <i>IL12A</i> ; <i>ICOSLG</i>
Interferon-Gamma Response	>0.001	<i>CD86</i> ; <i>CD274</i> ; <i>CDKN1A</i> ; <i>IL4R</i> ; <i>VCAM1</i> ; <i>IL10RA</i> ; <i>TNFAIP3</i> ; <i>NFKB1</i> ; <i>ICAM1</i> ; <i>NFKBIA</i> ; <i>IRF7</i> ; <i>STAT4</i> ; <i>TXNIP</i> ; <i>CCL2</i>
IL-2/STAT5 Signaling	>0.001	<i>CD86</i> ; <i>IL4R</i> ; <i>CSF1</i> ; <i>TNFRSF9</i> ; <i>IL10RA</i> ; <i>LIF</i> ; <i>ITGAE</i> ; <i>TNFRSF1B</i> ; <i>MAPKAPK2</i> ; <i>TNFSF11</i> ; <i>CTLA4</i> ; <i>ICOS</i> ; <i>CD44</i>
IL-6/JAK/STAT3 Signaling	>0.001	<i>CCR1</i> ; <i>IL4R</i> ; <i>CSF1</i> ; <i>TNFRSF12A</i> ; <i>IL1B</i> ; <i>TNFRSF1B</i> ; <i>CD44</i> ; <i>TNFRSF1A</i>
KRAS Signaling Up	>0.001	<i>PLAU</i> ; <i>ITGA2</i> ; <i>IL1B</i> ; <i>IL10RA</i> ; <i>LIF</i> ; <i>PLAUR</i> ; <i>TNFAIP3</i> ; <i>TNFRSF1B</i> ; <i>ETS1</i>

Table 3. Cont.

Term	Adjusted <i>p</i> -Value	Genes
Coagulation	>0.001	THBD; C8G; PLAUI; ITGA2; C8A; THBS1; SH2B2
Epithelial–Mesenchymal Transition	>0.001	VCAM1; TNFRSF12A; ITGA2; PLAUR; TNFAIP3; ITGA5; THBS1; CD44
Apical Junction	>0.001	CD86; CD274; VCAM1; ITGA2; ICAM4; CD34; ICAM1
Apoptosis	0.005	CDKN1A; TNFRSF12A; IL1B; TXNIP; CD44
Interferon-Alpha Response	0.005	IL4R; CSF1; IRF7; TXNIP
PanCancer		
TNF-alpha Signaling via NF-kB	>0.001	DUSP5; CDKN1A; GADD45A; LIF; TNFAIP3; ETS2; FOSL1; NR4A3; PLAUI; CLCF1; ID2; IL1B; MAP3K8
Epithelial–Mesenchymal Transition	>0.001	GADD45A; ITGA2; ID2; MMP3; TNFAIP3; LAMC2; THBS1; DKK1
KRAS Signaling Up	>0.001	PLAU; ITGA2; ID2; IL1B; LIF; TNFAIP3; PLAT; NGF
Coagulation	>0.001	PLAU; ITGA2; MMP3; PLAT; THBS1
Apoptosis	>0.001	CDKN1A; WEE1; GADD45A; IL1B; PLAT
Complement	>0.001	DUSP5; PIM1; TNFAIP3; GZMB; PLAT
p53 Pathway	>0.001	CDKN1A; GADD45A; LIF; SFN; EPHA2
IL-6/JAK/STAT3 Signaling	0.002	IL1B; PIM1; MAP3K8
IL-2/STAT5 Signaling	0.002	SPRY4; PIM1; LIF; MAP3K8
Inflammatory Response	0.002	CDKN1A; IL1B; LIF; OSM
Allograft Rejection	0.002	IL11; IL1B; LIF; GZMB
PI3K/AKT/mTOR Signaling	0.003	CDKN1A; SFN; NGF
TGF-beta Signaling	0.01	ID2; THBS1
Hypoxia	0.01	CDKN1A; PIM1; TNFAIP3
Estrogen Response Late	0.01	ID2; LAMC2; SFN
Interferon-Gamma Response	0.01	CDKN1A; PIM1; TNFAIP3
E2F Targets	0.01	CDKN1A; WEE1; HMGA1
Xenobiotic Metabolism	0.01	ID2; ETS2; EPHA2

3.3. Impact of ZEB1 and SNAI1 Expression on the Immune TME

To investigate whether tumors expressing high *ZEB1* and *SNAI1* levels affect the variation in immune cell composition in PCa, we investigated the relative abundance of immune cells using TCGA-PRAD public domain transcriptomic data. CIBERSORTx analysis was used to determine the impact of “high” vs. “low” expression levels of *ZEB1* and *SNAI1* on TILs and the immune content of the TME. Our results showed that *ZEB1*’s high expression was associated with an increased abundance of naïve B cells, resting memory CD4+ T cells, and M2 macrophages, and a decreased abundance of memory B cells, CD8 T cells, follicular T helper cells, monocytes, and M0 macrophages (Figure 4A), whilst *SNAI1*’s high expression showed an increased presence of dendritic and B cells (Figure 4B).

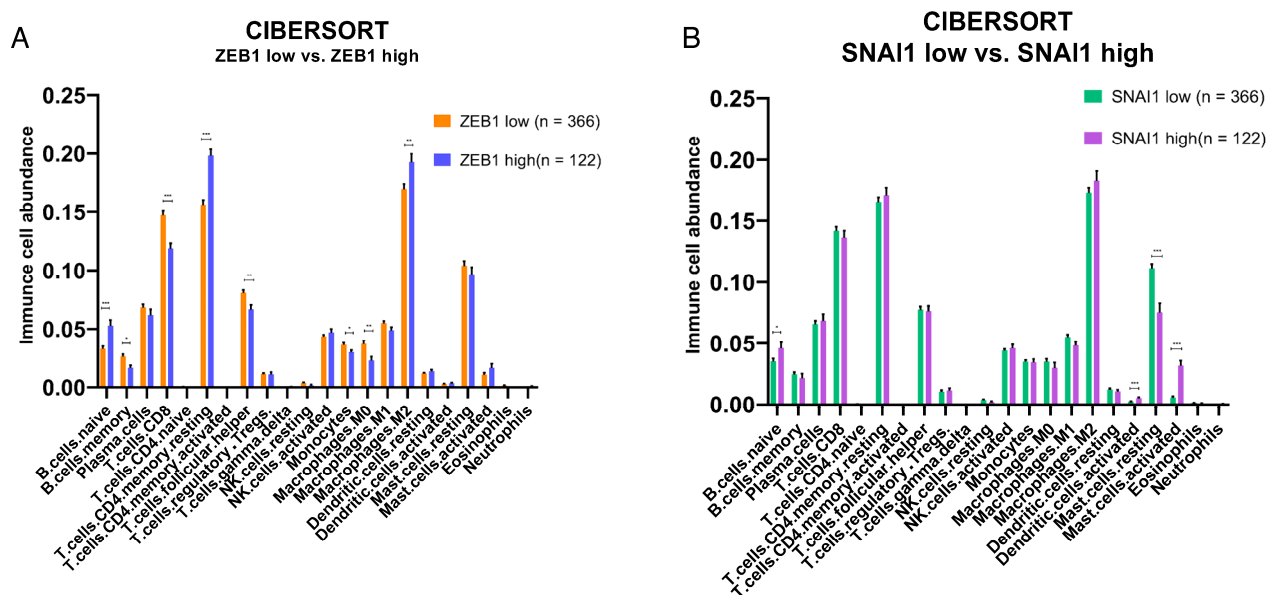


Figure 4. Effects of a high and low expression of EMT transcription factors on the relative abundance of immune cells in the TME of the PRAD-TCGA cohort. Deconvolution-based digital cytometry shows that expression levels of EMT transcription factors influence the relative abundance of immune cell content in the TME. **(A)** The high *ZEB1* group showed an increased abundance of naïve B cells, resting memory CD4+ T cells, and M2 macrophages, and a decreased abundance of memory B cells, CD8 T cells, follicular T helper cells, monocytes, and M0 macrophages. **(B)** *SNAI1* shows an increased abundance of naïve B cells, resting dendritic cells, and activated mast cells, and a decreased abundance of resting mast cells. Results derived from public domain data (TCGA-PRAD). * *p*-value < 0.05; ** *p*-value < 0.01; *** *p*-value < 0.001 by Mann–Whitney test.

The changes in the immune response in the TME associated with the altered expression of *ZEB1* and *SNAI1* suggested that these EMT-related transcription factors may directly or indirectly alter the expression of immune modulatory molecules. For example, we found that the expression of the checkpoint gene *CD274* (*PD-L1*) was associated with *SNAI1*'s high expression in our retrospective cohort analysis (Figure 3C,D). We, therefore, investigated whether the expression of *ZEB1* and *SNAI1* was also associated with changes in the expression of specific immune checkpoints and immune evasion-related markers in the TCGA-PRAD cohort. Our analysis showed that a high expression of the EMT transcription factors *ZEB1* and *SNAI1* is associated with an elevated expression of *CTLA-4*, *PD-L1*, *HAVCR2* (*TIM-3*), *DCR3*, and *IL10*, and *IL10RA* (Supplementary Figures S3 and S4), suggesting a pattern of the upregulation of immunomodulatory genes resulting in an increase in the composition of immune cells of the TME. Also, these findings collectively highlight the role of the TME in shaping the gene expression signature and outcome in PCa.

4. Discussion

An important hallmark of cancer is understanding how tumors manage to evade the host immune system [70]. This is a crucial adaptive advantage for survival, maintenance, and the evolution of cancer, especially after the emerging success of different types of immunotherapies. PCa is a tumor considered immunologically cold, that is, a type of tumor that is successful in immune evasion and, consequently, does not respond well to immunotherapy [7,8].

The dynamic and reversible nature of the EMT program impacts not only the tumor cells but also the surrounding ECM by accumulating immune suppressive cells in the TME and upregulating immunomodulatory molecules [22]. In PCa, EMT pathways have already been shown to be strongly related to characteristics of progression and aggressiveness, such as migration, invasion, and increased metastatic potential [14,18]. There is growing

evidence suggesting that a partial EMT phenotype, in which cells can simultaneously maintain both epithelial and mesenchymal characteristics, may lead to more aggressive disease than a complete EMT [69]. This observation is consistent with our finding that higher *ZEB1* expression was associated with a reduced risk of BCR.

Proteins in the collagen family play critical roles in diverse cellular processes, including cell adhesion, migration, differentiation, and proliferation. Collagens in the ECM can engage integrins on tumor cells, impede T cell infiltration, interact with CAFs, and facilitate invasion and metastasis [71]. Of the thirty-nine DEGs in our cohort significantly associated with BCR or CAPRA-S, we identified an increased expression of four collagen genes (*COL1A1*, *COL1A2*, *COL3A1*, and *COL5A2*). Of these, *COL3A1* (collagen type III alpha 1) is the most common DEG in our series, and it is an established biomarker of poor outcome in PCa [38,72]. Its expression also appears to promote immune infiltration in a wide variety of different cancers [73]. *COL3A1* interacts with fibronectin (*FN1*), which was also found to be significantly overexpressed. A crucial component of the ECM, *FN1*, is also intricately associated with collagens and CAFs [52]. Similarly, increased expression of *INHBA* (inhibin β A) was also observed from our results and is associated with enhanced collagen expression, including both *COL3A1* and *COL5A2* [74]. An increased expression of *COL3A1* in PCa activates other pro-tumorigenic genes and pathways, such as the Wnt/beta-catenin [38]. *COL3A1* expression is associated with higher Gleason scores, higher PSA levels, and a higher likelihood of lymph node involvement. Additionally, *COL5A2* expression correlated with increased tumor cell invasion and resistance to androgen deprivation therapy [40]. *SFRP2* was identified as a regulator of the TME through its impact on Wnt signaling and tumor angiogenesis [41,42], while *THBS4* influenced cancer stem cell-like properties in PCa via the PI3K/Akt pathway [43]. Several other DEGs have been previously associated with higher Gleason scores, including *COL1A2* and *INHBA* (subunit of Activin A) [44,45]. *WNT2B* is regulated by long non-coding RNAs (lncRNAs) and has been shown to play a role in influencing the EMT in PCa [46], while *SFRP4* emerged as a predictor of BCR in PCa, and its expression is also linked to the EMT [47].

Analysis of the immune-related components identified several DEGs that could be involved in shaping the immune landscape of PCa that were also associated with disease progression defined by CAPRA-S and BCR status (Table 2). The expression of Interferon Regulatory Factor 5 (*IRF5*) was associated with BCR, suggesting that this immune response modulator may also influence prognosis [58]. Similarly, the observation that *THY1* is overexpressed in PCa-associated fibroblasts may also be involved in antigen presentation in the stromal components of the TME of PCa [63]. The identification of *HLA-DRA* in our analysis offers the possibility that dysregulation may affect antigen presentation within the TME and influence the immune response [65]. *NRP* has been reported to be upregulated by androgen deprivation therapy (ADT) in advanced PCa [66], and its expression is thought to lead to increased vascularization and facilitate tumor progression. The co-expression of the immune cytokines *CXCL10* with *CXCR3* has been previously associated with metastatic recurrence [60].

It is noteworthy that of our 39 high-risk significantly associated DEGs, *ENG*, *INHBA*, *COL1A1*, *COL3A1*, *COL5A2*, *SFRP4*, *THY1*, and *CXCL14* were also identified as prognostic biomarkers in a recently published transcriptional signature predictive of recurrence [75]. *COL3A1*, *FN1*, and *THBS4* were found to be associated with high infiltration of Tregs in bone metastatic PCa [72]. Similarly, a recent patent identified *COL1A1*, *FN1*, *COL3A1*, *INHBA*, and *SFRP4* as stromal response genes that can be used to test for PCa outcome [76].

Eleven of the thirty-nine significant DEGs were identified as *ZEB1* target genes using the Harmonizome database [67]. Nine of the eleven *ZEB1* target genes were associated with high CAPRA-S. The proteins encoded by these 11 DEGs, *COL1A1*, *WNT2B*, *IRF5*, *SYK*, *BMP8A*, *NTRK1*, *JAG1*, *DNMT1*, *CD14*, *GAS1*, and *SIGIRR*, collectively present a set of functional properties that may be integral in limiting the immune response within the TME of PCa when an EMT transcriptional program is regulated by *ZEB1*. For example, collagen production by *COL1A1* may physically impede immune cell infiltration [77], while

WNT2B signaling is associated with immunosuppression [46]. IRF5, involved in immune regulation, and SYK, have been implicated in immune cell functions [59]. Additionally, BMP8A, NTRK1, JAG1, and GAS1 each bring unique contributions that can influence the immunosuppressive characteristics of the TME [49,51,53,54]. Furthermore, DNMT1 and CD14, through epigenetic regulation and immune cell activation, respectively, contribute to the overall immune evasion [78]. Lastly, SIGIRR's role as a negative regulator of Toll-like receptor signaling suggests its potential involvement in immune suppression [64].

Validation using the PRAD TCGA public cohort showed that both EMT drivers *ZEB1* and *SNAIL* are associated with the expression of the immunological evasion markers *CTLA-4*, *PD-L1*, *TIM3*, *DCR3*, and *IL10*. The expression of these markers leads not only to an inactivation of T cells but also to a generalized immune suppression in the TME [79]. Checkpoint proteins like CTLA-4 and PD-L1 inhibit T cell activation by delivering inhibitory signals to T cells upon engagement with their respective ligands. This inhibition prevents the full activation of T cells, leading to a state of quiescence where T cells remain inactive and are unable to mount an effective immune response against tumors [80].

Analysis of the relative abundance of immune cells in the TME of the PRAD TCGA cohort showed that *ZEB1* expression was associated with an increase in M2 polarization macrophages, which are known to be involved in the suppression of immunological activity [81]. Decreases in memory B cells, CD8+ T cells, follicular T helper cells, monocytes, and M0 macrophages further support *ZEB1* expression and may influence anti-tumor immunity in the TME and recruitment of TILs. In contrast, digital cytometric analysis of the effects of high *SNAIL* expression on the TME correlated with increased abundance of naïve B cells, resting dendritic cells, and activated mast cells, while showing decreased levels of resting mast cells. Interestingly, mast cell infiltration in PCa has been associated with chemotherapy resistance through the activation of p38/p53/p21 signaling [82]. Collectively, these data suggest that downstream changes activated by EMT transcription factors not only influence the aggressive behavior of tumors but also lead to changes in the immune activity of the TME.

5. Conclusions

In summary, these data suggest that the differential expression of collagen genes, such as *COL3A1* and various immune response genes observed in our study, are part of the EMT program, leading to cellular alterations that impact immune cell functions in the microenvironment of PCa. Collagen-related signals can modulate T cell activation, proliferation, and cytokine production. Moreover, the density and organization of collagen fibers could affect the spatial distribution and activation levels of immune cells within the tumor, influencing their ability to recognize and eliminate cancer cells. Understanding the interplay between the spatial effects of collagen and immune cells in the TME has therapeutic implications. This study has some limitations. The CAPRA-S score, which was used to classify the groups according to tumor progression relies on pathological factors, like the Gleason score and tumor stage. While these are important, they may not fully capture the complexity of prostate cancer biology and its interaction with the host environment. Furthermore, our sample size of 51 cases, while limited, was aimed at providing pilot data to establish a connection between the EMT and the immune TME in prostate cancer, thereby providing a basis for future clinical investigations with larger cohorts. This study suggests that future treatment strategies aimed at modulating the EMT [14,83] may enhance immune cell infiltration toward an anti-tumorigenic phenotype, which could be beneficial for countering immunotherapy resistance in a cold tumor, such as PCa.

Supplementary Materials: The following supporting information can be downloaded at <https://www.mdpi.com/article/10.3390/cancers16081480/s1>, Table S1: Prostate cancer tissue samples and validation cohort. BCR, biochemical recurrence; CAPRA-S, Cancer of the Prostate Risk Assessment Score; pGS, pathologic Gleason score; ISUP, International Society of Urological Pathology Score; TNM, Classification of Malignant Tumors. * For validation comparisons, we used RNA-seq data from

the prostate adenocarcinoma cohort from The Cancer Genome Atlas (PRAD-TCGA, $n = 420$) [36]. Table S2: Enrichment analysis from the DEGs associated with BCR and CAPRA-S in the FMRP cohort. List of ORA enriched analysis using MSigDb Hallmark's terms for DEGs associated with BCR and CAPRA-S using both the Immune Profile and PanCancer panels. Both comparisons used no BCR and low CAPRA-S scores as references from the FMRP cohort. Table S3: DEGs based on *ZEB1* and *SNAIL1*. List of DEGs from Immune Profiling and PanCancer panels for patients classified according to *ZEB1* and *SNAIL1* expression. The genes were considered DE when $\log_2 FC > 0.5$ and p -adjusted (FDR) < 0.05 . Table S4: Enrichment analysis from DEGs associated with a high *ZEB1* expression in the FMRP cohort. List of ORA-enriched pathways using MSigDb Hallmark's terms for DEGs associated with a high expression of *ZEB1*. The analysis used patients with a low expression of *ZEB1* as a reference. Figure S1: Correlation plots of common genes between Immune Profiling and PanCancer panels. Pearson correlation was used in normalized expression levels of each gene. The heatmap shows the Pearson correlation coefficient. Non-significant results are displayed in white and significant correlations are colored ($p < 0.01$). Figure S2: Summary workflow. We conducted NanoString panel profiling using RNA extracted from formalin-fixed paraffin-embedded (FFPE) tissues from the Faculty of Medicine of Ribeirão Preto (FMRP) cohort ($n = 51$). DEGs and pathway and downstream analyses of *ZEB1* and *SNAIL1* were performed using our in-house pipeline (see methods). Figure S3: Effects of a high and low *ZEB1* expression on the relative expression of checkpoint genes. Analysis of the expression of known immunomodulatory markers shows an increased relative expression of *CTLA-4*, *PD-L1*, *HAVCR2* (*TIM-3*), *IDO1*, *DCR3*, *IL10*, and *IL10RA* in the high *ZEB1* group ($n = 366$) compared to the low group ($n = 122$) in the TCGA cohort. * $p < 0.05$, Mann–Whitney test. Figure S4: Effects of a high and low *SNAIL1* expression on the relative expression of checkpoint genes. Analysis of the expression of known immunomodulatory markers shows an increased relative expression of *CTLA-4*, *PD-L1*, *HAVCR2* (*TIM-3*), *IDO1*, *DCR3*, *IL10*, and *IL10RA* in the high *SNAIL1* group ($n = 366$) compared to the low group ($n = 122$) in the TCGA cohort. * $p < 0.05$, Mann–Whitney test.

Author Contributions: L.P.C.: Conceptualization, data curation, investigation, methodology, project administration, visualization, and writing—review and editing. W.L.-D.: Conceptualization, data curation, formal analysis, investigation, methodology, project administration, validation, visualization, writing—original draft, and writing—review and editing. C.M.M.: Data curation, investigation, methodology, validation, and writing—review and editing. F.C.S.: Data curation and writing—review and editing. C.C.: Data curation, investigation, methodology, validation, and writing—review and editing. D.D.: Data curation, investigation, methodology, validation, and writing—review and editing. F.S.A.: Data curation, methodology, and writing—review and editing. F.P.S.: Data curation, investigation, methodology, validation, and writing—review and editing. R.B.d.R.: Data curation, investigation, methodology, project administration, and writing—review and editing. L.F.A.: Data curation, investigation, methodology, project administration, and writing—review and editing. J.B.: Conceptualization, data curation, formal analysis, funding acquisition, investigation, methodology, project administration, resources, supervision, validation, visualization, writing—original draft, and writing—review and editing. J.A.S.: Conceptualization, data curation, formal analysis, funding acquisition, investigation, methodology, project administration, resources, supervision, validation, visualization, writing—original draft, and writing—review and editing. All authors have read and agreed to the published version of the manuscript.

Funding: This work was supported by the Fundação de Amparo à Pesquisa do Estado de São Paulo (FAPESP) [grant numbers 2019/22912-8 to J.A.S., 2021/12816-9 (L.P.C.), 2021/12271-5 (W.L.-D.), and 2021/15011-4 to J.A.S., R.B.d.R. and L.F.A.], CNPq Bolsa de Produtividade em Pesquisa PQ-2019 308024/2019-2 (J.A.S.) and funds from the Government of Ontario to J.B.

Institutional Review Board Statement: This retrospective study was approved by the Ethics Committee in Research of Hospital of Ribeirão Preto, São Paulo, Brazil (HCRP) numbers CAAE 60032122.8.0000.5440 (13 July 2022), CAAE 43277221.0.0000.5440 (7 March 2022) and the Ethics Board of the University of Toronto (Protocol: 00043323, 13 September 2022). The studies were conducted in accordance with the local legislation and institutional requirements.

Informed Consent Statement: Informed consent was obtained from all subjects involved in the study.

Data Availability Statement: The datasets presented in this study can be found in online repositories. The names of the repository/repositories and accession number(s) can be found in the article/Supplementary Materials.

Acknowledgments: The authors acknowledge the contributions of the Department of Surgery and Anatomy, the Department of Pathology, FMRP-USP, and members of Diagnostic Development at the Ontario Institute for Cancer Research. We thank the patients for their contributions to the study.

Conflicts of Interest: J.B. has the patent application “A Molecular Classifier for Personalized Risk Stratification for Patients with Prostate Cancer” under consideration. Status: PCT, Filing Date: 18 June 2021, International Application No. PCT/CA2021/050837, PCT Application Title: Molecular Classifiers for Prostate Cancer. Previous US Provisional Status: Filing Date: 18 June 2020, US Provisional Patent No. 63/040.692, US Provisional Application Title: Use of Molecular Classifiers to Diagnose, Treat, and Prognose Prostate Cancer. The remaining authors declare that the research was conducted in the absence of any commercial or financial relationships that could be constructed as a potential conflict of interest.

References

1. Siegel, R.L.; Miller, K.D.; Wagle, N.S.; Jemal, A. Cancer statistics, 2023. *CA Cancer J. Clin.* **2023**, *73*, 17–48. [\[CrossRef\]](#)
2. Sung, H.; Ferlay, J.; Siegel, R.L.; Laversanne, M.; Soerjomataram, I.; Jemal, A.; Bray, F. Global Cancer Statistics 2020: GLOBOCAN Estimates of Incidence and Mortality Worldwide for 36 Cancers in 185 Countries. *CA Cancer J. Clin.* **2021**, *71*, 209–249. [\[CrossRef\]](#)
3. Rebello, R.J.; Oing, C.; Knudsen, K.E.; Loeb, S.; Johnson, D.C.; Reiter, R.E.; Gillissen, S.; Van der Kwast, T.; Bristow, R.G. Prostate cancer. *Nat. Rev. Dis. Prim.* **2021**, *7*, 9. [\[CrossRef\]](#)
4. Baciarello, G.; Gizzi, M.; Fizazi, K. Advancing therapies in metastatic castration-resistant prostate cancer. *Expert Opin. Pharmacother.* **2018**, *19*, 1797–1804. [\[CrossRef\]](#)
5. Abida, W.; Cheng, M.L.; Armenia, J.; Middha, S.; Autio, K.A.; Vargas, H.A.; Rathkopf, D.; Morris, M.J.; Danila, D.C.; Slovin, S.F.; et al. Analysis of the Prevalence of Microsatellite Instability in Prostate Cancer and Response to Immune Checkpoint Blockade. *JAMA Oncol.* **2019**, *5*, 471–478. [\[CrossRef\]](#)
6. Wu, Y.M.; Cieřlik, M.; Lonigro, R.J.; Vats, P.; Reimers, M.A.; Cao, X.; Ning, Y.; Wang, L.; Kunju, L.P.; de Sarkar, N.; et al. Inactivation of CDK12 Delineates a Distinct Immunogenic Class of Advanced Prostate Cancer. *Cell* **2018**, *173*, 1770–1782.e14. [\[CrossRef\]](#)
7. Melo, C.M.; Vidotto, T.; Chaves, L.P.; Lautert-Dutra, W.; Dos Reis, R.B.; Squire, J.A. The role of somatic mutations on the immune response of the tumor microenvironment in prostate cancer. *Int. J. Mol. Sci.* **2021**, *22*, 9550. [\[CrossRef\]](#)
8. Stultz, J.; Fong, L. How to turn up the heat on the cold immune microenvironment of metastatic prostate cancer. *Prostate Cancer Prostatic Dis.* **2021**, *24*, 697–717. [\[CrossRef\]](#)
9. Fridman, W.H.; Pagès, F.; Sautès-Fridman, C.; Galon, J. The immune contexture in human tumours: Impact on clinical outcome. *Nat. Rev. Cancer* **2012**, *12*, 298–306. [\[CrossRef\]](#)
10. Nardone, V.; Botta, C.; Caraglia, M.; Martino, E.C.; Ambrosio, M.R.; Carfagno, T.; Tini, P.; Semeraro, L.; Misso, G.; Grimaldi, A.; et al. Tumor infiltrating T lymphocytes expressing FoxP3, CCR7 or PD-1 predict the outcome of prostate cancer patients subjected to salvage radiotherapy after biochemical relapse. *Cancer Biol. Ther.* **2016**, *17*, 1213–1220. [\[CrossRef\]](#)
11. Zhao, S.G.; Lehrer, J.; Chang, S.L.; Das, R.; Erho, N.; Liu, Y.; Sjöström, M.; Den, R.B.; Freedland, S.J.; Klein, E.A.; et al. The immune landscape of prostate cancer and nomination of PD-L2 as a potential therapeutic target. *J. Natl. Cancer Inst.* **2019**, *111*, 301–310. [\[CrossRef\]](#)
12. Ge, R.; Wang, Z.; Cheng, L. Tumor microenvironment heterogeneity an important mediator of prostate cancer progression and therapeutic resistance. *NPJ Precis. Oncol.* **2022**, *6*, 31. [\[CrossRef\]](#)
13. Haffner, M.C.; Zwart, W.; Roudier, M.P.; True, L.D.; Nelson, W.G.; Epstein, J.I.; De Marzo, A.M.; Nelson, P.S.; Yegnasubramanian, S. Genomic and phenotypic heterogeneity in prostate cancer. *Nat. Rev. Urol.* **2021**, *18*, 79–92. [\[CrossRef\]](#)
14. Brabletz, S.; Schuhwerk, H.; Brabletz, T.; Stemmler, M.P. Dynamic EMT: A multi-tool for tumor progression. *EMBO J.* **2021**, *40*, e108647. [\[CrossRef\]](#)
15. Derynck, R.; Weinberg, R.A. EMT and Cancer: More Than Meets the Eye. *Dev. Cell* **2019**, *49*, 313–316. [\[CrossRef\]](#)
16. Stemmler, M.P.; Eccles, R.L.; Brabletz, S.; Brabletz, T. Non-redundant functions of EMT-TFs. *Nat. Cell Biol.* **2019**, *21*, 102–112. [\[CrossRef\]](#)
17. Orellana-Serradell, O.; Herrera, D.; Castellon, E.A.; Contreras, H.R. The transcription factor ZEB1 promotes an aggressive phenotype in prostate cancer cell lines. *Asian J. Androl.* **2018**, *20*, 294–299. [\[CrossRef\]](#)
18. Stylianou, N.; Lehman, M.L.; Wang, C.; Fard, A.T.; Rockstroh, A.; Fazli, L.; Jovanovic, L.; Ward, M.; Sadowski, M.C.; Kashyap, A.S.; et al. A molecular portrait of epithelial–mesenchymal plasticity in prostate cancer associated with clinical outcome. *Oncogene* **2019**, *38*, 913–934. [\[CrossRef\]](#)
19. Poblete, C.E.; Fulla, J.; Gallardo, M.; Muñoz, V.; Castellón, E.A.; Gallegos, I.; Contreras, H.R. Increased SNAIL expression and low syndecan levels are associated with high Gleason grade in prostate cancer. *Int. J. Oncol.* **2014**, *44*, 647–654. [\[CrossRef\]](#)
20. Neal, C.L.; Henderson, V.; Smith, B.N.; McKeithen, D.; Graham, T.; Vo, B.T.; Odero-Marah, V.A. Snail transcription factor negatively regulates maspin tumor suppressor in human prostate cancer cells. *BMC Cancer* **2012**, *12*, 336. [\[CrossRef\]](#)

21. Horn, L.A.; Fousek, K.; Palena, C. Tumor Plasticity and Resistance to Immunotherapy. *Trends Cancer* **2020**, *6*, 432–441. [[CrossRef](#)] [[PubMed](#)]
22. Taki, M.; Abiko, K.; Ukita, M.; Murakami, R.; Yamanoi, K.; Yamaguchi, K.; Hamanishi, J.; Baba, T.; Matsumura, N.; Mandai, M. Tumor immune microenvironment during epithelial- mesenchymal transition. *Clin. Cancer Res.* **2021**, *27*, 4669–4679. [[CrossRef](#)] [[PubMed](#)]
23. Pickup, M.; Novitskiy, S.; Moses, H.L. The roles of TGF β in the tumour microenvironment. *Nat. Rev. Cancer* **2013**, *13*, 788–799. [[CrossRef](#)] [[PubMed](#)]
24. Suzuki, H.I. MicroRNA control of TGF- β signaling. *Int. J. Mol. Sci.* **2018**, *19*, 1901. [[CrossRef](#)] [[PubMed](#)]
25. Zhang, J.; Tian, X.J.; Zhang, H.; Teng, Y.; Li, R.; Bai, F.; Elankumaran, S.; Xing, J. TGF- β -induced epithelial-to-mesenchymal transition proceeds through stepwise activation of multiple feedback loops. *Sci. Signal.* **2014**, *7*, ra91. [[CrossRef](#)] [[PubMed](#)]
26. Terry, S.; Savagner, P.; Ortiz-Cuaran, S.; Mahjoubi, L.; Saintigny, P.; Thiery, J.P.; Chouaib, S. New insights into the role of EMT in tumor immune escape. *Mol. Oncol.* **2017**, *11*, 824–846. [[CrossRef](#)] [[PubMed](#)]
27. Mohler, J.L.; Antonarakis, E.S.; Armstrong, A.J.; D’Amico, A.V.; Davis, B.J.; Dorff, T.; Eastham, J.A.; Enke, C.A.; Farrington, T.A.; Higano, C.S.; et al. Prostate Cancer, Version 2.2019, NCCN Clinical Practice Guidelines in Oncology. *J. Natl. Compr. Canc. Netw.* **2019**, *17*, 479–505. [[CrossRef](#)] [[PubMed](#)]
28. Lautert-Dutra, W.; Melo, C.M.; Chaves, L.P.; Souza, F.C.; Crozier, C.; Sundby, A.E.; Woroszczuk, E.; Saggioro, F.P.; Avante, F.S.; dos Reis, R.B.; et al. Identification of tumor-agnostic biomarkers for predicting prostate cancer progression and biochemical recurrence. *Front. Oncol.* **2023**, *13*, 1280943. [[CrossRef](#)]
29. Cooperberg, M.R.; Hilton, J.F.; Carroll, P.R. The CAPRA-S score: A straightforward tool for improved prediction of outcomes after radical prostatectomy. *Cancer* **2011**, *22*, 5039–5046. [[CrossRef](#)]
30. Bayani, J.; Yao, C.Q.; Quintayo, M.A.; Yan, F.; Haider, S.; DCosta, A.; Brookes, C.L.; Van De Velde, C.J.H.; Hasenburg, A.; Kieback, D.G.; et al. Molecular stratification of early breast cancer identifies drug targets to drive stratified medicine. *NPJ Breast Cancer* **2017**, *3*, 3. [[CrossRef](#)]
31. Patel, P.G.; Selvarajah, S.; Guérard, K.P.; Bartlett, J.M.S.; Lapointe, J.; Berman, D.M.; Okello, J.B.A.; Park, P.C. Reliability and performance of commercial RNA and DNA extraction kits for FFPE tissue cores. *PLoS ONE* **2017**, *12*, 0179732. [[CrossRef](#)]
32. Goytain, A.; Ng, T. NanoString nCounter Technology: High-Throughput RNA Validation. In *Chimeric RNA. Methods in Molecular Biology*; Li, H., Elfman, J., Eds.; Humana: New York, NY, USA, 2020; pp. 125–139. ISBN 978-1-4939-9903-3.
33. Olkhov-Mitsel, E.; Hodgson, A.; Liu, S.K.; Vesprini, D.; Bayani, J.; Bartlett, J.; Xu, B.; Downes, M.R. Immune gene expression profiles in high-grade urothelial carcinoma of the bladder: A NanoString study. *J. Clin. Pathol.* **2021**, *74*, 53–57. [[CrossRef](#)] [[PubMed](#)]
34. Love, M.I.; Huber, W.; Anders, S. Moderated estimation of fold change and dispersion for RNA-seq data with DESeq2. *Genome Biol.* **2014**, *15*, 550. [[CrossRef](#)]
35. Wu, T.; Hu, E.; Xu, S.; Chen, M.; Guo, P.; Dai, Z.; Feng, T.; Zhou, L.; Tang, W.; Zhan, L.; et al. clusterProfiler 4.0: A universal enrichment tool for interpreting omics data. *Innovation* **2021**, *2*, 100141. [[CrossRef](#)]
36. Thorsson, V.; Gibbs, D.L.; Brown, S.D.; Wolf, D.; Bortone, D.S.; Ou Yang, T.H.; Porta-Pardo, E.; Gao, G.F.; Plaisier, C.L.; Eddy, J.A.; et al. The Immune Landscape of Cancer. *Immunity* **2018**, *48*, 812–830.e14. [[CrossRef](#)] [[PubMed](#)]
37. Chen, B.; Khodadoust, M.S.; Liu, C.L.; Newman, A.M.; Alizadeh, A.A. Profiling tumor infiltrating immune cells with CIBERSORT. *Methods Mol. Biol.* **2018**, *1711*, 243–259. [[CrossRef](#)] [[PubMed](#)]
38. Angel, P.M.; Spruill, L.; Jefferson, M.; Bethard, J.R.; Ball, L.E.; Hughes-Halbert, C.; Drake, R.R. Zonal regulation of collagen-type proteins and posttranslational modifications in prostatic benign and cancer tissues by imaging mass spectrometry. *Prostate* **2020**, *80*, 1071–1086. [[CrossRef](#)]
39. Szabo, P.M.; Vajdi, A.; Kumar, N.; Tolstorukov, M.Y.; Chen, B.J.; Edwards, R.; Ligon, K.L.; Chasalow, S.D.; Chow, K.H.; Shetty, A.; et al. Cancer-associated fibroblasts are the main contributors to epithelial-to-mesenchymal signatures in the tumor microenvironment. *Sci. Rep.* **2023**, *13*, 3051. [[CrossRef](#)] [[PubMed](#)]
40. Georgescu, I.; Gooding, R.J.; Doiron, R.C.; Day, A.; Selvarajah, S.; Davidson, C.; Berman, D.M.; Park, P.C. Molecular characterization of Gleason patterns 3 and 4 prostate cancer using reverse Warburg effect-associated genes. *Cancer Metab.* **2016**, *4*, 8. [[CrossRef](#)]
41. Sun, Y.; Zhu, D.; Chen, F.; Qian, M.; Wei, H.; Chen, W.; Xu, J. SFRP2 augments WNT16B signaling to promote therapeutic resistance in the damaged tumor microenvironment. *Oncogene* **2016**, *35*, 4321–4334. [[CrossRef](#)]
42. van Loon, K.; Huijbers, E.J.M.; Griffioen, A.W. Secreted frizzled-related protein 2: A key player in noncanonical Wnt signaling and tumor angiogenesis. *Cancer Metast. Rev.* **2021**, *40*, 191–203. [[CrossRef](#)] [[PubMed](#)]
43. Hou, Y.; Li, H.; Huo, W. THBS4 silencing regulates the cancer stem cell-like properties in prostate cancer via blocking the PI3K/Akt pathway. *Prostate* **2020**, *80*, 753–763. [[CrossRef](#)] [[PubMed](#)]
44. Chen, L.; De Menna, M.; Groenewoud, A.; Thalmann, G.N.; Kruithof-de Julio, M.; Snaar-Jagalska, B.E. A NF- κ B-Activin A signaling axis enhances prostate cancer metastasis. *Oncogene* **2020**, *39*, 1634–1651. [[CrossRef](#)] [[PubMed](#)]
45. Reader, K.L.; John-McHaffie, S.; Zellhuber-McMillan, S.; Jowett, T.; Mottershead, D.G.; Cunliffe, H.E.; Gold, E.J. Activin B and Activin C Have Opposing Effects on Prostate Cancer Progression and Cell Growth. *Cancers* **2023**, *15*, 147. [[CrossRef](#)] [[PubMed](#)]
46. Han, Y.; Hu, H.; Zhou, J. Knockdown of LncRNA SNHG7 inhibited epithelial-mesenchymal transition in prostate cancer through miR-324-3p/WNT2B axis in vitro. *Pathol. Res. Pract.* **2019**, *215*, 152537. [[CrossRef](#)] [[PubMed](#)]

47. Yimamu, Y.; Yang, X.; Chen, J.; Luo, C.; Xiao, W.; Guan, H.; Wang, D. The Development of a Gleason Score-Related Gene Signature for Predicting the Prognosis of Prostate Cancer. *J. Clin. Med.* **2022**, *11*, 7164. [\[CrossRef\]](#) [\[PubMed\]](#)
48. Qing, Y.; Wang, Y.; Hu, C.; Zhang, H.; Huang, Y.; Zhang, Z.; Ma, T.; Zhang, S.; Li, K. Evaluation of NOTCH family genes' expression and prognostic value in prostate cancer. *Transl. Androl. Urol.* **2022**, *11*, 627–642. [\[CrossRef\]](#)
49. Liu, B.; Li, X.; Li, J.; Jin, H.; Jia, H.; Ge, X. Construction and Validation of a Robust Cancer Stem Cell-Associated Gene Set-Based Signature to Predict Early Biochemical Recurrence in Prostate Cancer. *Dis. Markers* **2020**, *2020*, 8860788. [\[CrossRef\]](#)
50. Karanika, S.; Karantanos, T.; Li, L.; Wang, J.; Park, S.; Yang, G.; Zuo, X.; Song, J.H.; Maity, S.N.; Manyam, G.C.; et al. Targeting DNA Damage Response in Prostate Cancer by Inhibiting Androgen Receptor-CDC6-ATR-Chk1 Signaling. *Cell Rep.* **2017**, *18*, 1970–1981. [\[CrossRef\]](#)
51. Bagherabadi, A.; Hooshmand, A.; Shekari, N.; Singh, P.; Zolghadri, S.; Stanek, A.; Dohare, R. Correlation of NTRK1 Downregulation with Low Levels of Tumor-Infiltrating Immune Cells and Poor Prognosis of Prostate Cancer Revealed by Gene Network Analysis. *Genes* **2022**, *13*, 840. [\[CrossRef\]](#)
52. Erdogan, B.; Ao, M.; White, L.M.; Means, A.L.; Brewer, B.M.; Yang, L.; Washington, M.K.; Shi, C.; Franco, O.E.; Weaver, A.M.; et al. Cancer-associated fibroblasts promote directional cancer cell migration by aligning fibronectin. *J. Cell Biol.* **2017**, *216*, 3799–3816. [\[CrossRef\]](#)
53. Su, Q.; Zhang, B.; Zhang, L.; Dang, T.; Rowley, D.; Ittmann, M.; Xin, L. Jagged1 upregulation in prostate epithelial cells promotes formation of reactive stroma in the Pten null mouse model for prostate cancer. *Oncogene* **2017**, *36*, 618–627. [\[CrossRef\]](#) [\[PubMed\]](#)
54. Xiong, Z.; Ge, Y.; Xiao, J.; Wang, Y.; Li, L.; Ma, S.; Lan, L.; Liu, B.; Qin, B.; Luan, Y.; et al. GAS1RR, an immune-related enhancer RNA, is related to biochemical recurrence-free survival in prostate cancer. *Exp. Biol. Med.* **2023**, *248*, 1–13. [\[CrossRef\]](#) [\[PubMed\]](#)
55. Du, Z.; Li, L.; Sun, W.; Zhu, P.; Cheng, S.; Yang, X.; Luo, C.; Yu, X.; Wu, X. Systematic Evaluation for the Influences of the SOX17/Notch Receptor Family Members on Reversing Enzalutamide Resistance in Castration-Resistant Prostate Cancer Cells. *Front. Oncol.* **2021**, *11*, 607291. [\[CrossRef\]](#) [\[PubMed\]](#)
56. Vidal, A.C.; Duong, F.; Howard, L.E.; Wiggins, E.; Freedland, S.J.; Bhowmick, N.A.; Gong, J. Soluble endoglin (sCD105) as a novel biomarker for detecting aggressive prostate cancer. *Anticancer Res.* **2020**, *40*, 1459–1462. [\[CrossRef\]](#) [\[PubMed\]](#)
57. Williams, K.A.; Lee, M.; Hu, Y.; Andreas, J.; Patel, S.J.; Zhang, S.; Chines, P.; Elkahloun, A.; Chandrasekharappa, S.; Gutkind, J.S.; et al. A Systems Genetics Approach Identifies CXCL14, ITGAX, and LPCAT2 as Novel Aggressive Prostate Cancer Susceptibility Genes. *PLoS Genet.* **2014**, *10*, e1004809. [\[CrossRef\]](#) [\[PubMed\]](#)
58. Lv, D.; Wu, X.; Chen, X.; Yang, S.; Chen, W.; Wang, M.; Liu, Y.; Gu, D.; Zeng, G. A novel immune-related gene-based prognostic signature to predict biochemical recurrence in patients with prostate cancer after radical prostatectomy. *Cancer Immunol. Immunother.* **2021**, *70*, 3587–3602. [\[CrossRef\]](#) [\[PubMed\]](#)
59. Ghotra, V.P.S.; He, S.; Van Der Horst, G.; Nijhoff, S.; De Bont, H.; Lekkerkerker, A.; Janssen, R.; Jenster, G.; Van Leenders, G.J.L.H.; Hoogland, A.M.M.; et al. SYK is a candidate kinase target for the treatment of advanced prostate cancer. *Cancer Res.* **2015**, *75*, 230–240. [\[CrossRef\]](#) [\[PubMed\]](#)
60. Wightman, S.C.; Uppal, A.; Pitroda, S.P.; Ganai, S.; Burnette, B.; Stack, M.; Oshima, G.; Khan, S.; Huang, X.; Posner, M.C.; et al. Oncogenic CXCL10 signalling drives metastasis development and poor clinical outcome. *Br. J. Cancer* **2015**, *113*, 327–335. [\[CrossRef\]](#)
61. Long, X.; Wu, L.; Zeng, X.; Wu, Z.; Hu, X.; Jiang, H.; Lv, Z.; Yang, C.; Cai, Y.; Yang, K.; et al. Biomarkers in previous histologically negative prostate biopsies can be helpful in repeat biopsy decision-making processes. *Cancer Med.* **2020**, *9*, 7524–7536. [\[CrossRef\]](#)
62. Debska-Zielkowska, J.; Moszkowska, G.; Zieliński, M.; Zielińska, H.; Dukat-Mazurek, A.; Trzonkowski, P.; Stefańska, K. KIR Receptors as Key Regulators of NK Cells Activity in Health and Disease. *Cells* **2021**, *10*, 1777. [\[CrossRef\]](#)
63. True, L.D.; Zhang, H.; Ye, M.; Huang, C.Y.; Nelson, P.S.; Von Haller, P.D.; Tjoelker, L.W.; Kim, J.S.; Qian, W.J.; Smith, R.D.; et al. CD90/THY1 is overexpressed in prostate cancer-associated fibroblasts and could serve as a cancer biomarker. *Mod. Pathol.* **2010**, *23*, 1346–1356. [\[CrossRef\]](#)
64. Bauman, T.M.; Becka, A.J.; Sehgal, P.D.; Huang, W.; Ricke, W.A. SIGIRR/TIR8, an important regulator of TLR4 and IL-1R-mediated NF- κ B activation, predicts biochemical recurrence after prostatectomy in low-grade prostate carcinomas. *Hum. Pathol.* **2015**, *46*, 1744–1751. [\[CrossRef\]](#)
65. Tuerff, D.; Muller, D.J.; Lap, C.J.G.; Liu, S.; Diao, G.; Antonio, M.; Nava, V.; Jain, M.R. The association of HLA-DR and PD-L1 expression with clinical characteristics in prostate. *J. Clin. Oncol.* **2023**, *41*, 17017. [\[CrossRef\]](#)
66. Tse, B.W.C.; Volpert, M.; Ratther, E.; Stylianou, N.; Nouri, M.; McGowan, K.; Lehman, M.L.; McPherson, S.J.; Roshan-Moniri, M.; Butler, M.S.; et al. Neuropilin-1 is upregulated in the adaptive response of prostate tumors to androgen-targeted therapies and is prognostic of metastatic progression and patient mortality. *Oncogene* **2017**, *36*, 3417–3427. [\[CrossRef\]](#)
67. Rouillard, A.D.; Gundersen, G.W.; Fernandez, N.F.; Wang, Z.; Monteiro, C.D.; McDermott, M.G.; Ma'ayan, A. The harmonizome: A collection of processed datasets gathered to serve and mine knowledge about genes and proteins. *Database* **2016**, *2016*, baw100. [\[CrossRef\]](#) [\[PubMed\]](#)
68. Chaves, L.P.; Melo, C.M.; Saggiaro, F.P.; Borges, R.; Squire, J.A. Epithelial—Mesenchymal Transition Signaling and Prostate Precision Therapeutics. *Genes* **2021**, *12*, 1900. [\[CrossRef\]](#)
69. Kitz, J.; Lefebvre, C.; Carlos, J.; Lowes, L.E.; Allan, A.L. Reduced zeb1 expression in prostate cancer cells leads to an aggressive partial-emt phenotype associated with altered global methylation patterns. *Int. J. Mol. Sci.* **2021**, *22*, 12840. [\[CrossRef\]](#)
70. Hanahan, D. Hallmarks of Cancer: New Dimensions. *Cancer Discov.* **2022**, *12*, 31–46. [\[CrossRef\]](#) [\[PubMed\]](#)

71. Cox, T.R. The matrix in cancer. *Nat. Rev. Cancer* **2021**, *21*, 217–238. [[CrossRef](#)]
72. Meng, F.; Han, X.; Min, Z.; He, X.; Zhu, S. Prognostic signatures associated with high infiltration of Tregs in bone metastatic prostate cancer. *Aging* **2021**, *13*, 17442–17461. [[CrossRef](#)] [[PubMed](#)]
73. Zhang, H.; Ding, C.; Li, Y.; Xing, C.; Wang, S.; Yu, Z.; Chen, L.; Li, P.; Dai, M. Data mining-based study of collagen type III alpha 1 (COL3A1) prognostic value and immune exploration in pan-cancer. *Bioengineered* **2021**, *12*, 3634–3646. [[CrossRef](#)] [[PubMed](#)]
74. Nagaraja, A.S.; Dood, R.L.; Armaiz-Pena, G.; Kang, Y.; Wu, S.Y.; Allen, J.K.; Jennings, N.B.; Mangala, L.S.; Pradeep, S.; Lyons, Y.; et al. Adrenergic-mediated increases in INHBA drive CAF phenotype and collagens. *JCI Insight* **2017**, *2*, e93076. [[CrossRef](#)] [[PubMed](#)]
75. Li, X.; Huang, H.; Zhang, J.; Jiang, F.; Guo, Y.; Shi, Y.; Guo, Z.; Ao, L. A qualitative transcriptional signature for predicting the biochemical recurrence risk of prostate cancer patients after radical prostatectomy. *Prostate* **2020**, *80*, 376–387. [[CrossRef](#)] [[PubMed](#)]
76. Shak, S.; Lee, M.; Novotny, W.; Maddala, T.; Crager, M.; Cherbavaz, D.; Pelham, R.; Millward, C.L.; Knezevic, D. Gene Expression Profile Algorithm and Test for Determining Prognosis of Prostate Cancer. AU2018201688A1, 27 February 2020.
77. Yin, W.; Zhu, H.; Tan, J.; Xin, Z.; Zhou, Q.; Cao, Y.; Wu, Z.; Wang, L.; Zhao, M.; Jiang, X.; et al. Identification of collagen genes related to immune infiltration and epithelial-mesenchymal transition in glioma. *Cancer Cell Int.* **2021**, *21*, 276. [[CrossRef](#)] [[PubMed](#)]
78. Lee, E.; Wang, J.; Yumoto, K.; Jung, Y.; Cackowski, F.C.; Decker, A.M.; Li, Y.; Franceschi, R.T.; Pienta, K.J.; Taichman, R.S. DNMT1 Regulates Epithelial-Mesenchymal Transition and Cancer Stem Cells, Which Promotes Prostate Cancer Metastasis. *Neoplasia* **2016**, *18*, 553–566. [[CrossRef](#)] [[PubMed](#)]
79. Khalil, D.N.; Smith, E.L.; Brentjens, R.J.; Wolchok, J.D. The future of cancer treatment: Immunomodulation, CARs and combination immunotherapy. *Nat. Rev. Clin. Oncol.* **2016**, *13*, 273–290. [[CrossRef](#)] [[PubMed](#)]
80. Renaude, E.; Kroemer, M.; Borg, C.; Peixoto, P.; Hervouet, E.; Loyon, R.; Adotévi, O. Epigenetic Reprogramming of CD4+ Helper T Cells as a Strategy to Improve Anticancer Immunotherapy. *Front. Immunol.* **2021**, *12*, 669992. [[CrossRef](#)]
81. Erlandsson, A.; Carlsson, J.; Lundholm, M.; Fält, A.; Andersson, S.O.; Andrén, O.; Davidsson, S. M2 macrophages and regulatory T cells in lethal prostate cancer. *Prostate* **2019**, *79*, 363–369. [[CrossRef](#)]
82. Xie, H.; Li, C.; Dang, Q.; Chang, L.S.; Li, L. Infiltrating mast cells increase prostate cancer chemotherapy and radiotherapy resistances via modulation of p38/p53/p21 and ATM signals. *Oncotarget* **2016**, *7*, 1341–1353. [[CrossRef](#)]
83. Huang, Y.; Hong, W.; Wei, X. The molecular mechanisms and therapeutic strategies of EMT in tumor progression and metastasis. *J. Hematol. Oncol.* **2022**, *15*, 129. [[CrossRef](#)] [[PubMed](#)]

Disclaimer/Publisher’s Note: The statements, opinions and data contained in all publications are solely those of the individual author(s) and contributor(s) and not of MDPI and/or the editor(s). MDPI and/or the editor(s) disclaim responsibility for any injury to people or property resulting from any ideas, methods, instructions or products referred to in the content.